FRACTURE TOUGHNESS EVALUATION OF COMPOSITE/METAL ADHESIVE STRUCTURE IN CRYOGENIC ENVIRONMENT

Ryohei Maruyama*, Tomohiro Yokozeki **, Toshio Ogasawara* , Takeshi Ogawa***
*** Aoyamagakuin University, **The University of Tokyo,**
***** Japan Aerospace Exploration Agency**

Keywords: *Adhesive, Thermal Residual Stress, Fracture Toughness, DCB test*

Abstract

The evaluation of adhesive fracture characteristics is important to enhance the safety and the reliability of composite/metal adhesive structures. In this study, an analytical method is presented for the evaluation of the correct adhesive fracture toughness including the effect of thermal residual stresses in the case of symmetric and asymmetric adhesive DCB tests. Because of the temperature change and the difference of thermal expansion between adherends and adhesives, the resultant residual thermal stresses induce bending moments in the test specimen, and thus, this effect is incorporated in the present method to evaluate the fracture mechanics properties accurately. Material properties are experimentally measured for evaluation of residual thermal stress, and the present method is validated by experimental verification tests. Finally, the experimental results of the adhesive fracture toughness at cryogenic temperature are presented, and the present correction methodology is demonstrated.

1 Introduction

The development of CFRP tank structures with Al alloy liner has been attempted for light-weight cryogenic fuel storage system of space launch vehicles [1]. However, the onset of debondings between CFRP and Al liner was reported during the structural test. It has been considered that the misfit of thermal shrinkage among CFRP, Al alloy, and adhesives results in this composite tank failure. Severe thermal residual stresses are induced in the tank structures due to the difference in coefficients of thermal expansion (CTEs) between the adherends and the adhesives when there exist differences between the molding temperature and the service temperature [2]. The fracture characteristics evaluation of the adhesive bonded structures is important to advance the safety and the reliability of cryogenic composite tanks [3].

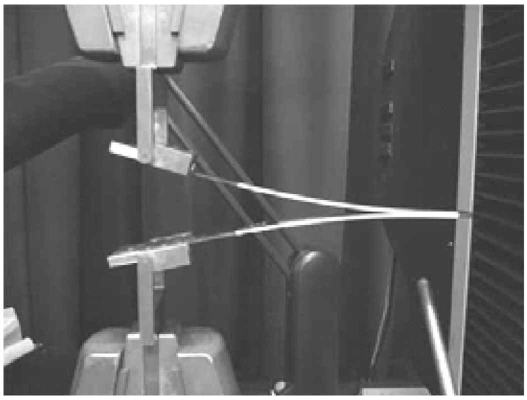

Fig. 1. Double cantilever beam (DCB) test

Double cantilever beam (DCB) tests (Fig.1) is enumerated as standard evaluation tests of the fracture mechanics characteristics in the bonded structures (e.g. JIS and ASTM). However, these standards do not include the effect of thermal residual stresses. It is necessary to consider the effect of thermal residual stresses on the evaluation of fracture toughness [4], specifically under a low temperature environment, where the influence may become much remarkable. Nairn also showed the necessity of the correction for this problem [4]. He derived the correction method that includes the influence of thermal residual stress in the energy release rates of DCB specimens which have identical upper and lower adherends, and crack progressing at the center of the adhesive (i.e. symmetric DCB specimens) [4].

In this study, an analytical method is presented for the evaluation of the correct adhesive fracture toughness including the effect of thermal residual stresses in the case of DCB test. This method is validated by experimental verification tests, and the material characterizations are measured by the experiment for evaluating thermal residual stress. Finally, DCB test was performed using composite materials/aluminum alloy bonded specimens that simulated composite tank structures with metal liners. Further more the experimental results on the adhesive fracture toughness at cryogenic temperature are presented, and the present correction methodology is applied. Methodology and experimental results on the accurate evaluation of adhesive fracture toughness is presented in this study, which is considered to contribute the development of the reliable metal-liner composite tank structures.

2 Correction method for adhesive fracture toughness

2.1Correction method [5]

The authors [5] described an analytical expression for the relation between the apparent fracture toughness and the true fracture toughness of adhesive DCB specimens subjected to residual thermal stresses as shown in Eq. (1) using the multilayer beam model, in which the upper and the lower adherends are different. As shown in Fig.2, the upper part of the cracked arm is denoted as area <1>, the lower part is area <2>, and the intact part of the beam is area <3>.

$$G_C = G_C^{app} + \frac{Pa}{B}\left(F^{\langle 1\rangle} + F^{\langle 2\rangle}\right)\ \Delta T + \frac{1}{2}\left(I^{\langle 1\rangle} + I^{\langle 2\rangle} + I^{\langle 3\rangle}\right) \qquad (1)$$

Here, G_C^{app} is the apparent fracture toughness (without thermal residual stresses) and it can be considered to be a value obtained from the DCB test result. And F and I are constants obtained from the lamination theory.

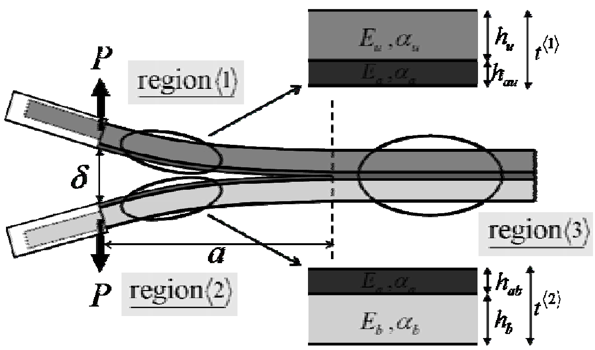

Fig. 2 Evaluation method of fracture toughness

2.2 Verification

2.2.1 Comparison with FEM results

Verification of the correction method was conducted by the comparison with the FEM result. The FEM model used in this section was a symmetric adhesive DCB specimen, as shown in Fig. 3. In FEM models, SiC-FRP(tyranno A / #1063EX) was used for the adherend, and AF163-2K was used for the adhesive. The DCB specimens were modeled using plane stress elements, and the analysis was performed using ABAQUS Ver. 6.5. VCCT (virtual crack closure technique) was used for the evaluation of energy release rates [6]. The stress-free temperature was set to be 130℃, and temperature was fluctuated down to -150℃, which was the test temperature. In the FEM analysis, only mechanical loads (without temperature change) and both temperature change and mechanical loads were applied for evaluating the apparent energy release rate (G_C^{app}) and true energy release rate (G), respectively. The crack length was set to be 87.5 mm. The applied load was set to be 2.19 N per width (mm) of the specimen. Two cases when the crack grows in the middle plane of the adhesive layer (symmetric crack growth) and when it grows at SiC-FRP/Adhesive interface (asymmetric crack growth) were analyzed. For comparison, correction based on Nairn's formulation [4] was also conducted for the case of symmetric crack growth.

The corrected result is shown in Table 1. It can be concluded that the corrected result using the present method agrees well with the result of FEM for both cased of symmetric and asymmetric crack growth, and the effectiveness of this correction method is verified.

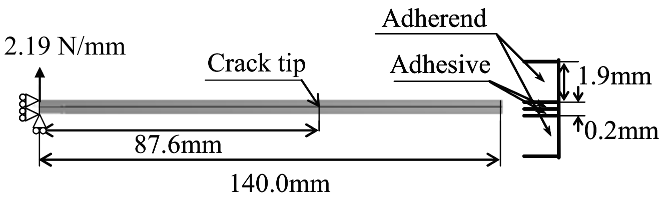

Fig.3 FEM model of DCB test

Table 1 Comparison with FEM analysis

	SiC-FRP / Adhesive	Inner adhesive
$G_C{}^{app}$	0.801	0.810
FEM G_C	0.760	0.768
Nairn correction [3] G_C	—	0.758
Correction used this study G_C	0.758	0.761

2.2.2 Experimental verification test

The presented method is verified experimentally in this section. The DCB specimens with different thermal residual stresses are subjected to DCB tests, and it is investigated whether the fracture toughness can be corrected by applying the correction method. The material used in this section was IM600/#133 (Toho Tenax), and three kinds of CFRP laminates ($[0_{24}]$, $[90_{12}/0_{12}]$ and $[90_{18}/0_6]$) were prepared. Using adhesive epoxy films (AF163-2K, 3M), the fabricated laminates were bonded in the manner that adhesive layers were placed between 0^o layers (e.g. $[90_{12}/0_{12}/\text{adhesive}/0_{12}/90_{12}]$), and specimens were cured at 130^{o}C for 2 h using a hot press and vacuum bag (Fig.4). The sizes of the specimens were 150mm length and 12.5mm width. Table 2 shows material properties of CFRP (referred to the document [7]) and adhesive (measured as described in section 3). Teflon sheets were partly placed between the adhesive and CFRP in order to induce initial delamination. The tests were carried out at room temperature (23℃) according to JIS K7086 (JIS: Japan Industrial Standards).

The tested specimens ($[0_{24}]$ and $[90_{18}/0_6]$) were shown in Fig.5. It can be confirmed for laminate specimen of $[90_{18}/0_6]$ that the edge side has been already open. Test results (apparent fracture toughness vs. crack growth) were shown in Fig.6. Though it is presumed that three kinds of test specimens show almost the identical fracture toughness because the adhesive configuration (e.g. bonded surfaces) and condition are same, the apparent fracture toughnesses of $[90_{12}/0_{12}]$ and $[90_{18}/0_6]$ laminate specimens were about 30% and 44% smaller than that of $[0_{24}]$ laminate specimen. However, when the present correction method was applied to the experimental results, the corrected fracture toughnesses exhibit similar values (within 10% errors) for all cases as shown in Fig. 7. Note that the corrected results coincide well with those based on Nairn [4]. Therefore, the validity of the correction method was also experimentally confirmed.

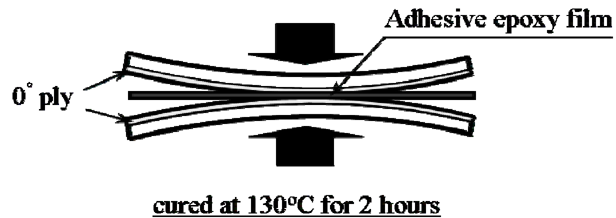

Fig. 4 Fabrication of verification test

Table 2 Material properties (23℃)

Material	CFRP[7] (IM600/#133)	Adhesive (AF163-2K)
E [GPa]	153.0	2.8
α [10^{-6}/ ℃]	-0.51	38.13

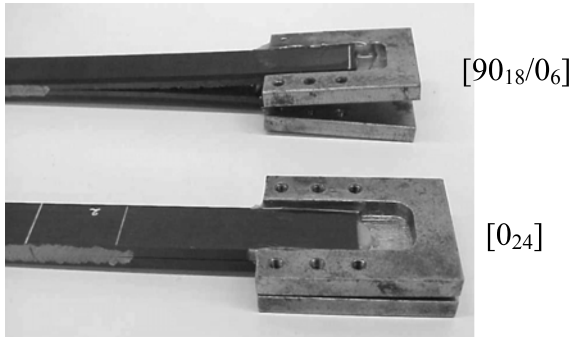

Fig. 5 Appearance of tested specimens

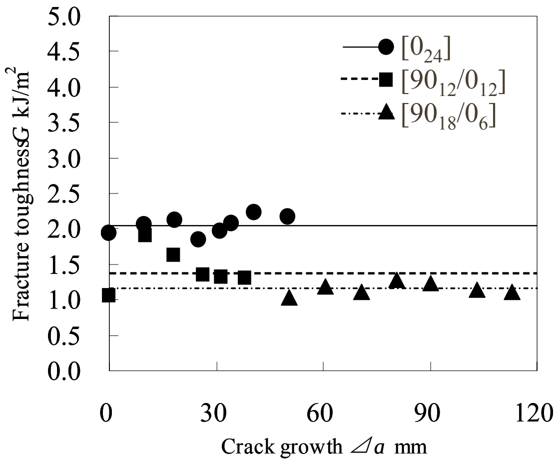

Fig. 6 Verification test result

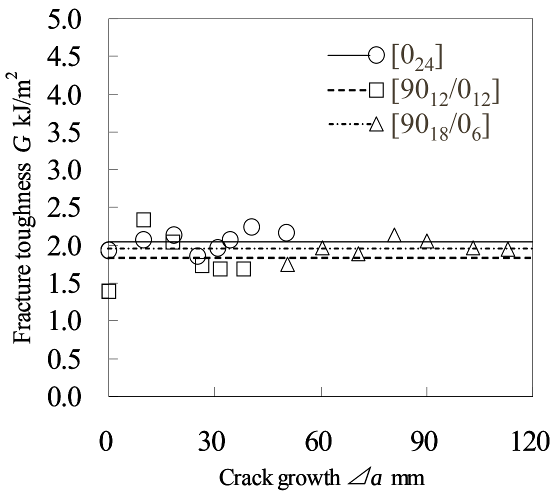

Fig. 7 Correction of verification test result

3 Experimental procedure

3.1 Mechanical properties

Mechanical properties are necessary for evaluation of the thermal residual stress and strain. Materials used in this study were CFRP(MR50 /#1063EX, $[0]_{16}$, Mitsubishi Rayon Japan), SiC-FRP (Tyranno A, Ube Industries / #1063EX, $[0]_{16}$), A6061-T6, and adhesive films (AF163-2K,3M). #1063EX is tough epoxy resin for the aircraft made by Mitsubishi Rayon Japan. Tension tests were conducted according to JIS Z 2241, K 7113, and K7073 at 23 ℃ (room temperature) and -196 ℃ (specimens were soaked in LN_2). In order to measure the shear modulus, mechanical properties (E_{45} and ν_{45}) measured using 45 ° test specimens were utilized according to the following equation [8].

$$G = \frac{E_{45}}{\{2(1+\nu_{45})\}} \qquad (2)$$

3.2 Thermal expansion

Thermal expansion behavior was evaluated using a laser dilatometer LIX-1 (ULVAC-RIKO) (Fig.8). Fig.9 showed the conformation of LIX-1. After filling liquid nitrogen in a thermostatic chamber, temperature increased at a constant heating rate. The displacement ΔL and the temperature T of test specimen were measured. The thermal strain ε was calculated from initial length L and ΔL, and the liner (tangential) coefficient of thermal expansion α was calculated from ε and ΔT. The heating rate of temperature change was set to be 1.0 ℃/min. Moreover, mean coefficient of thermal expansion α' at 23 ℃ and -150 ℃ was calculated by using the obtained linear thermal expansion coefficient and the trapezoidal method under the condition that stress free temperature is assumed to be the molding temperature, 130 ℃.

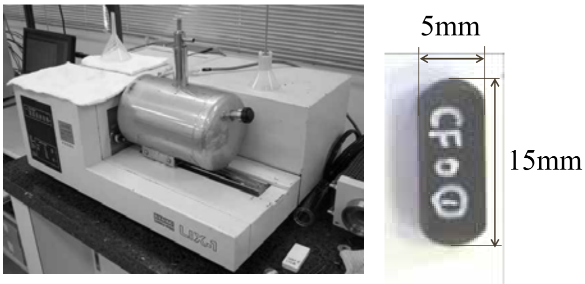

Fig.8 Laser dilatometer LIX-1 (ULVAC-RIKO) and Thermal expansion test specimen

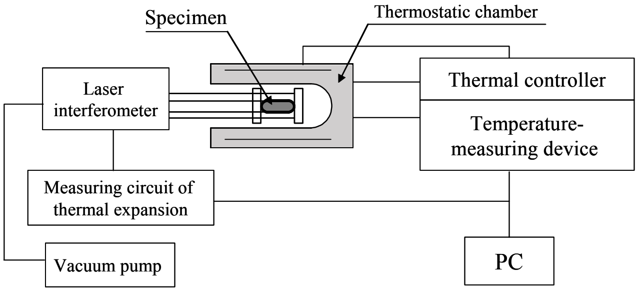

Fig.9 Conformation of LIX-1

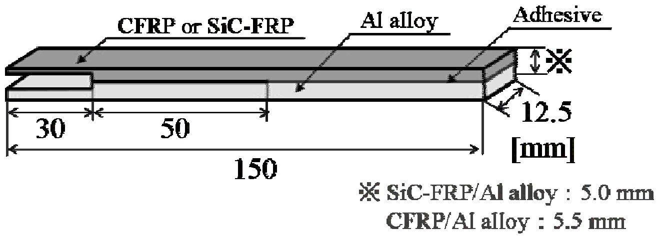

Fig.10 Adhesive DCB test specimen
(FRP 0 ° /Adhesive/Al alloy)

3.3 Adhesive fracture toughness

In this section, fracture mechanics characterization of FRP/metal adhesive structures is presented. FRP/metal adhesive structures are considered to be subjected to severe residual thermal stresses under cryogenic conditions. Experimental characterization of adhesive fracture toughness is performed combined with the present correction method. DCB tests were performed according to the standard (JIS K7086, ASTM D3433). The initial cracks were introduced using release films, and specimens were cured at 130°C. The specimens were subjected to the vertical load P, at a crosshead speed of 0.5 or 1mm/min using a mechanically driven machine. The displacement of the crosshead was used as the crack opening displacement (COD). The compliance method was used to evaluate the apparent fracture toughness in this study.

The specimen configuration is shown in Fig.10. The DCB tests were performed using composite materials/aluminum alloy bonded specimens that imitate composite tank structures with metal liners. The tests were conducted at room temperature and at -196℃. Two kinds of composite materials (CFRP and SiC-FRP) were prepared. The specimen size was set to be 150mm in length and 12.5mm in width. CFRP (MR50 / #1063EX), SiC-FRP (tyranno A / #1063EX), and Al alloy (A6061-T6) were used for the adherend. AF163-2K was used for the adhesive. Asymmetric DCB specimens with different adherends (e.g. FRP upper adherend and Al alloy lower adherend) were prepared, and the adhesive fracture toughness was evaluated.

4 Result and discussion

4.1 Mechanical properties and thermal expansion

Test results were shown Table 3 and 4, which suggest that CFRP is stiffer than SiC-FRP in 0° direction but the latter have higher 90° stiffness than the former. The CTE of CFRP is low in 0° direction compared to that of SiC-FRP. Therefore, it can be concluded that the CTE difference between CFRP and A6061-T6 (and AF163-2K) is significant compared to that between SiC-FRP and A6061-T6 (and AF163-2K). The thermal residual stress is expected to become large when CFRP is used for cryogenic metal-lined tank structures because the difference of the Young's modulus is also significant.

4.2 Adhesive fracture toughness and correction results

The load-COD curves obtained from the experiments were shown in Fig.11 and 12. The crack growth was observed at the interface between FRP and adhesive (FRP/Adhesive interface) at the -196°C, while the crack propagated in the adhesive layer at 23 °C. The stick-slip phenomenon was observed at cryogenic temperature, whereas stable crack growth was observed at room temperature. The stick-slip phenomenon was especially significant in CFRP/Al alloy specimens at -196°C. Therefore, the fracture toughness of CFRP/Al alloy specimens at -196°C was able to be acquired only at an initial stage of the crack growth. The correction method was applied to the obtained apparent fracture toughness. The crack growth in the adhesive layer was observed at 23°C. And the crack growth at the interface between FRP and adhesive was observed at -196°C. The results were shown in Fig. 13, 14, 15 and 16. In the graphs, the apparent fracture toughness obtained from experiment and corrected result is denoted as G_C^{app} and G_C, respectively. Here, the stress free temperature was assumed to be 130°C that was the molding temperature of the test specimen in the correction.

The corrected result, G_C, was higher than the apparent fracture toughness, G_C^{app}, in all cases in this section. In asymmetric DCB specimens examined in this section, energy release rates due to temperature change (the third term in equation (1)) are relatively large, and are dominant for the correction. The difference between G_C, and G_C^{app} is 1-3% at 23°C in both asymmetric DCB specimens. However, there is significant difference (more than twice) between G_C and G_C^{app} at -196°C. It is thought that the difference of thermal strain had been induced due to high temperature difference and the rigidity of each material increased at cryogenic temperature. Especially, it turned out that the influence was large for the CFRP/Al alloy test specimen. Therefore, it is concluded that the effect of residual thermal stress on the fracture toughness evaluation should be corrected at cryogenic temperature. It will be necessary to develop a correction method for other fracture mechanics tests (e.g. end-notched flexure) of adhesive structures such as cryogenic composite tanks.

Table 3 Material properties (23°C)

Material		SiC-FRP (TyrannoA/#1063EX)	CFRP (MR50/#1063EX)	Adhesive (AF163-2K)	Al alloy (A6061-T6)
E [GPa]	0°	89.8	163.1	2.8	69.8
	90°	13.5	8.7		
G [GPa]		4.12	4.5		
ν	0°	0.28	0.33	0.32	0.33
	90°	0.05	0.02		
α [10^{-6}/ °C]	0°	2.18	-0.02	38.13	18.67
	90°	14.01	—		

Table 4 Material properties (α:-150°C, Others:-196°C)

Material		SiC-FRP (TyrannoA/#1063EX)	CFRP (MR50/#1063EX)	Adhesive (AF163-2K)	Al alloy (A6061-T6)
E [GPa]	0°	88.1	161.3	9.7	77.1
	90°	28.6	12.7		
G [GPa]		10.8	12.6		
ν	0°	0.28	0.35	0.44	0.35
	90°	0.09	0.02		
α [10^{-6}/ °C]	0°	0.28	-0.19	25.97	15.55
	90°	14.01	—		

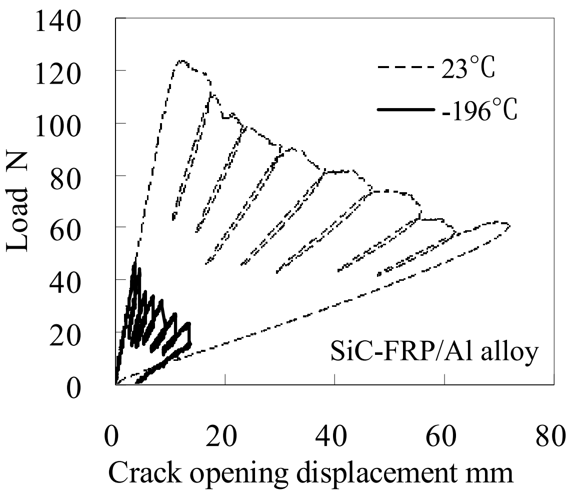

Fig.11 Load-COD plot by SiC-FRP/Al alloy

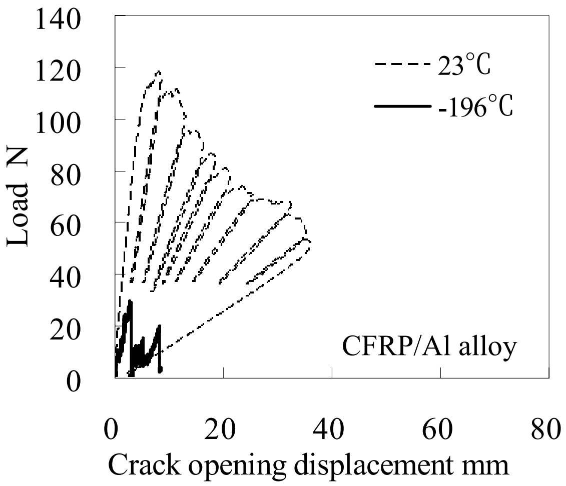

Fig.12 Load-COD plot by CFRP/Al alloy

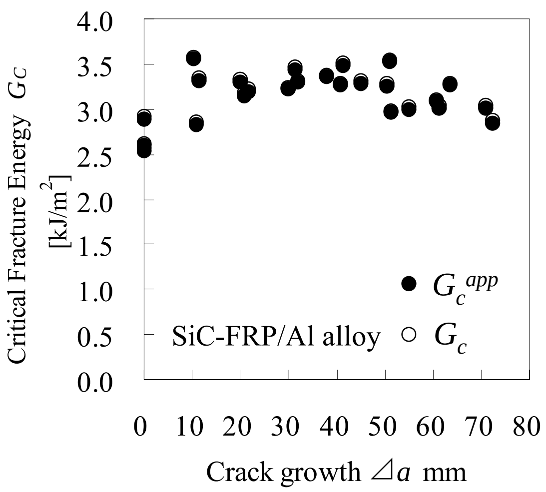

Fig.13 Fracture toughness of SiC-FRP/Al alloy (23°C)

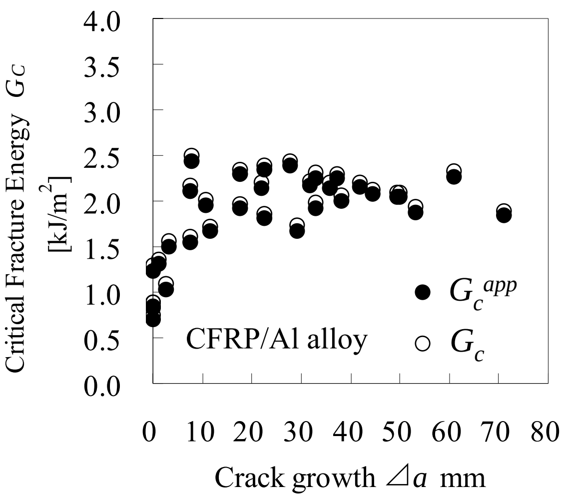

Fig.14 Fracture toughness of CFRP/Al alloy (23°C)

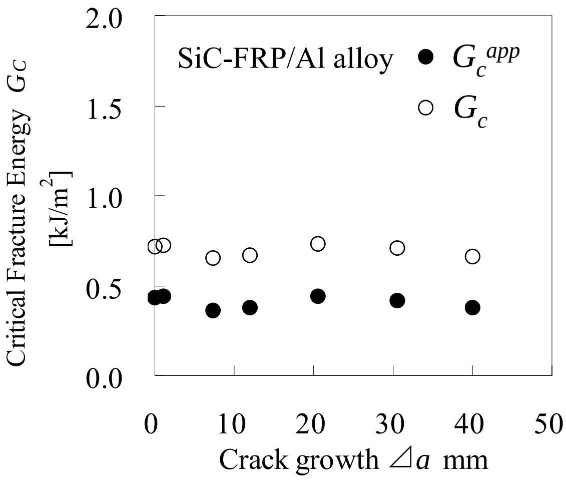

Fig.15 Fracture toughness of SiC-FRP/Al alloy (-196°C)

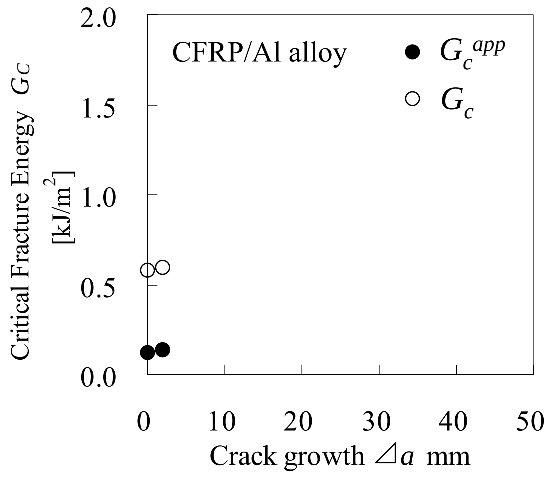

Fig.16 Fracture toughness of CFRP/Al alloy (-196°C)

4.3 Influence of the crack plane position and the adhesive thickness

The effect of crack plane position (e.g. crack at interface or crack in the adhesive layer) on the corrected fracture toughness is investigated in this section, because the corrected results depend on the position of crack plane. Three cases (crack growth at SiC-FRP/adhesive interface, crack growth in the middle plane of adhesive layer, and crack growth at Al alloy/adhesive interface) are examined, and the comparative results are shown in Table 4. It was demonstrated that the corrected values depend on the crack position (about 15%) at -196^{o}C, while the crack position has little influence on the fracture toughness evaluation at 23^{o}C. Therefore, observation of crack growth position is necessary for correcting the fracture toughness accurately.

Table 4 The effect by difference of crack growth position (SiC-FRP/Al alloy)

	SiC-FRP/Adhesive Interface	middle plane of adhesive layer	Al alloy/Adhesive Interface
23℃	3.290	3.300	3.297
-196℃	0.694	0.609	0.651

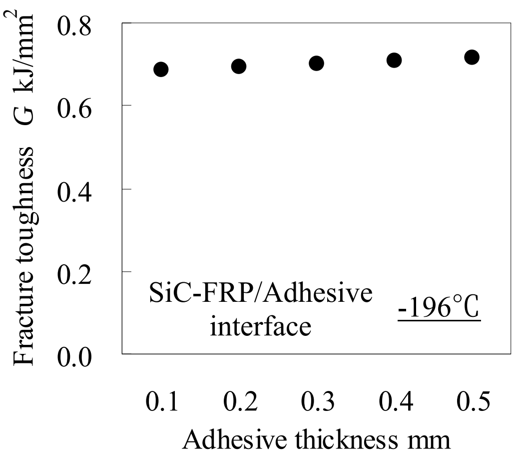

Fig.17 The effect by adhesive thickness (SiC-FRP/Al alloy)

When the specimens were bonded, the adhesive thickness was not uniform, nor locally identical to the measured value. Therefore, the effect of adhesive thickness on the corrected fracture toughness (or sensitivity of adhesive thickness) is investigated, herein, in the case of SiC-FRP/Al alloy specimens at cryogenic temperature. The thickness was changed from 0.1mm to 0.5mm.

The result when the crack was located at SiC-FRP/adhesive interface was shown in Fig.17. Comparison of the results between the cases of 0.1mm thickness and 0.5mm thickness indicates that the corrected value of the latter is about 5% higher than that of the former. It is concluded that the effect of adhesive thickness is small within the cases of thin adhesive thickness.

5 Conclusions

(1) Verification of the present correction method for measurement of true fracture toughness (with thermal residual stress) was conducted by comparison with FEM result, and demonstrated by experimental verification test. As a result, the validity of the correction method was confirmed.

(2) Material properties related to metal-lined composite tank structures were measured. The thermal residual stress is expected to become large when CFRP is used for cryogenic metal-lined tank structures because the difference of Young's modulus and CTE between CFRP and Al alloy (and also adhesive) is significant.

(3) The difference between the apparent fracture toughness and the true fracture toughness was significant at -196°C, and it was confirmed that the effect of residual thermal stresses on the evaluation of adhesive fracture toughness should be corrected for accurate measurement of adhesive fracture toughness, especially under cryogenic environment.

References

[1] Torano Y, Arita M, Takahashi H, Arima K, Namiki F, 10th International Space Planes and Hypersonic Systems and Technologies Conference, AIAA-2001-1877, 2001

[2] Suemasu H., Maeda Y., Namiki M., Proceeding of the JSASS/JSME Structure Conference, Vol.47, 2005, pp.60-62.

[3] J.He, Aoki T, Shimoda T, Proceeding of the JSASS/JSME Structure Conference, Vol.46, 2004, pp.158-160.

[4] J.A.Nairn, International Journal of Adhesion and Adhesive, Vol.20, 2000, pp.59-70

[5] Yokozeki T.,Maruyama R.,Ogasawara T., Proceeding of the 48th JSASS/JSME Structure Conference, 2006, pp.282-284

[6] Rybicki,E.F. and Kamminen.M.F. A finite element calculation of stress intensity factors by a modified crack closure integral Engineering Fracture Mechanics Vol.9, 1977, pp.931-938

[7] Aoki T, Ishikawa T, Kumazawa H, Morino Y Cryogenic mechanical properties of CF/polymer composites for tanks of reusable rockets Advanced Composite Materials Vol.10, No.4, 2001, pp.349-356

[8] Ishikawa T, Introduction to composite materials mechanics 1997, pp.8-13